

# Study on Morphology of High Impact Polypropylene Prepared by In Situ Blending

Tao Jiang, Hongxia Chen, Yingnan Ning, Dongting Kuang, Guangmiao Qu

Department of Chemical Engineering, Daqing Petroleum Institute, Daqing 163318, People's Republic of China

Received 10 April 2005; accepted 6 July 2005

DOI 10.1002/app.22581

Published online 27 April 2006 in Wiley InterScience (www.interscience.wiley.com).

**ABSTRACT:** High impact polypropylene (HIPP) was prepared by in situ blending of isotactic polypropylene and ethylene-propylene rubber (EPR) with spherical Ziegler-Natta catalyst. Morphology and pore characteristics of such HIPP were investigated by scanning electron microscope, atomic force microscopy, and mercury intrusion. Amorphous phase was removed from polypropylene matrix and characterized by  $^{13}\text{C}$  NMR spectrum. It was found that the EPR prepared in this manner contained variable composition polymer chains with a distribution of ethylene and propylene sequence lengths. Final products of HIPP were free flowing, spherical granules. There were small pores in

HIPP, which seemed not to be filled up, and could be determined by mercury intrusion even when the content of rubber was up to 24 wt %. Homopolypropylene with pore diameter between 100 and 10,000 nm was suitable for EPR to fill in during ethylene-propylene copolymerization. The block copolymer fractions act as a compatilizer between matrix and EPR. © 2006 Wiley Periodicals, Inc. *J Appl Polym Sci* 101: 1386–1390, 2006

**Key words:** morphology; high impact polypropylene; in situ blending; Ziegler-Natta polymerization

## INTRODUCTION

With improved low-temperature impact properties, high impact polypropylene (HIPP) has been found to have a variety of applications where the strength and impact resistance of polymer material were desired such as molded and extruded automobile parts, household appliances, luggage, and furniture.<sup>1</sup> HIPP is often prepared by mechanical blending of isotactic polypropylene (*i*-PP) and ethylene-propylene rubber (EPR) or by in situ blending technique. A typical in situ blending is a sequential polymerization process wherein the homopolypropylene produced in the first reactor is transferred to a second reactor where ethylene-propylene copolymer is prepared and incorporated into the matrix of the homopolymer component.<sup>2</sup> Therefore, the structure, morphology, and properties of spherical HIPP are expected to be different from those of traditional blends. The copolymer component has rubbery characteristics and provides the desired impact resistance, whereas the homopolymer component provides overall stiffness. The in situ blend has been proved to be superior both in mechanical properties and production costs.<sup>3</sup> Multiple-steps technologies were employed in the industrial process for HIPP: such as Spheripol (Basell), Unipol (UCC), Novolen (Targor), Hypol (Mitsui), Amoco, etc.<sup>4</sup> The

chain structure and property of HIPP prepared by multistage polymerization with spherical Ziegler-Natta catalyst have been studied by several researchers.<sup>5–7</sup> However, there are a few studies on morphology of HIPP, which can give important information about the interface of matrix and rubber.<sup>8–11</sup> In this article, the morphology and pore characterization of *i*-PP/EPR prepared by in situ blending via a spherical  $\text{TiCl}_4/\text{MgCl}_2$  catalyst were studied by using scanning electron microscope (SEM), atomic force microscopy (AFM), and mercury intrusion.

## EXPERIMENTAL

### Materials

All manipulations were carried out under an inert atmosphere of  $\text{N}_2$ , polymerization-grade propylene, ethylene, and high purity nitrogen were obtained from Daqing Petrochemical Co., Ltd., used after passage through 4 Å molecular sieve. Triethylaluminum (TEA), cyclohexylmethyldimethoxysilane (CHMDMS), *n*-hexane, and commercial Ziegler-Natta catalyst were supplied by Beijing Research Institute of Chemical Industry and used as received. The content of the titanium in the catalyst was 2.34 wt %, determined by 722 spectrophotometer. Particle size analysis results showed that the  $D_{50}$  of the catalyst was 48.3  $\mu\text{m}$ . The total specific surface area of the catalyst was 286.5  $\text{m}^2/\text{g}$  and total pore volume was 0.39  $\text{mL}/\text{g}$ , obtained from nitrogen adsorption measurements (Carlo Erba Strumentazione, Sorptomatic 1800).

Correspondence to: T. Jiang (jiangtao@dqpi.net).

### Preparation of *i*-PP/EPR in situ blend

The HIPP was synthesized in a two-stage reaction process in which the first stage was homopolymerization in liquid propylene at 70°C, and 10 mg commercial Ziegler–Natta catalyst was used, TEA as cocatalyst and CHMDMS as external under the conditions of Al/Ti molar ratio = 200 and Al/Si molar ratio = 20. The second stage was a successive gas-phase ethylene–propylene copolymerization in a stirred-bed reactor at 0.8 MPa. Porous spherical *i*-PP was produced in the first stage and transferred to the second reactor for copolymerization after removing the residual propylene in the particles completely. In the second stage, an ethylene–propylene mixture of constant ratio was continuously fed to the gas-phase reactor at constant pressure to run the copolymerization and in situ blending. Ethylene content of the in situ blend can be adjusted by varying the polymerization conditions.

### Characterization of polymer morphology and composition

Fourier-transfer infrared spectra of the HIPP were recorded on a Nicolet 5DX FTIR spectrometer. An empirical equation was employed to calculate the ethylene content in HIPP based on IR spectrum:  $\ln A_{1150}/A_{720} = 2.98 - 0.06 \times C_2$  ( $C_2$ —mole percent of ethylene in the polymer).<sup>12</sup> The characteristics of pore on the HIPP were determined by mercury intrusion (Micromeritics, Autopore 9410). AFM images were recorded with a Nanoscope III multimode AFM (Digital Instruments) operated in air in a tapping mode. The surface and section morphology of the polymer was examined in a SEM (model DSM-960). Section samples had been cryogenically fractured in liquid nitrogen at –60°C. The HIPP was dissolved in xylene at 135°C for 1 h and the resulting solution was cooled down to give crystallized PP. Then, the mixture was centrifuged at 25°C and the supernatant liquid was separated and evaporated to give EPR. The <sup>13</sup>C NMR spectrum was recorded on a Bruker DMX400 spectrometer operating at 100 MHz under proton noise decoupling in Fourier transform mode. Instrumental condition was as follows: pulse angle 90°, pulse repetition 2 s, spectral width 180 ppm, scans ~25,000, temperature 383 K, data points 64 K. The notched Izod impact strength of the polymer sample was measured on a Ceast impact strength tester, according to ASTM D 256. The flexural

TABLE I  
Composition of the Copolymer

	HIPP
Melt index (g/10 min)	30.28
Ethylene content (wt %)	14.00
Soluble in xylene (wt %)	24.01

TABLE II  
Triad Distribution of EPR

Triads	Percent (wt %)
PEP	9.41
PEE-EEP	13.25
EEE	8.59
EPE	10.38
PPE-EPP	27.35
PPP	31.02

modulus was measured following ASTM D 790 on a Shimadzu AG-500A electronic tester. The polymer granules were heat molded at 170°C into sheets, which were then cut into pieces, and pressed under 25 MPa at 180°C for 5 min. The sample plates were then slowly cooled to room temperature in the mold. Sample strips for the tests were cut from the plate following ASTM. For each test point, five parallel measurements were made and the average values were adopted.

## RESULTS AND DISCUSSION

### Composition, characterization, and mechanical property of HIPP

To know the microstructure and chemical composition of resulted HIPP, xylene extraction of such polymer blend was carried out and a <sup>13</sup>C NMR analysis of EPR was performed. Tables I and II show the chemical composition of HIPP and the triad distribution of EPR, respectively. <sup>13</sup>C NMR spectra of xylene-soluble fractions are shown in Figure 1. The E/P sequence distributions were calculated according to literature.<sup>13</sup> The mechanical properties of the HIPP and common PP were given in Table III. The results presented in Table III seem to show that tensile strength, flexural strength, flexural modulus, and rockwell hardness decreased and impact strength increased, as compared

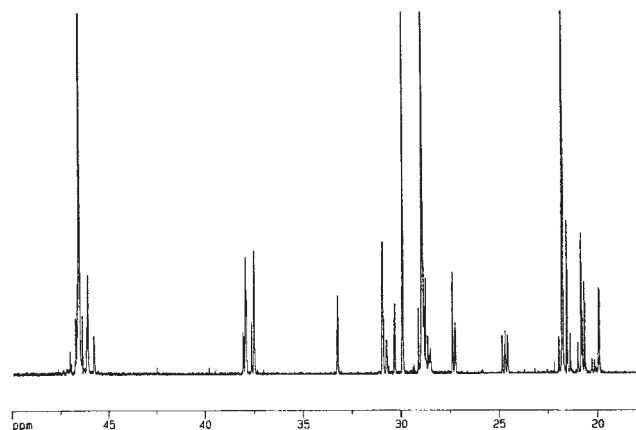


Figure 1 100 MHz <sup>13</sup>C NMR spectra of xylene-soluble fractions.

TABLE III

Typical property	HIPP	PP	Standard test methods
Izod impact (J/m)			
23°C	115	63	ASTMD 256-02
-20°C	79.6	23.2	ASTMD 256-02
Tensile strength (MPa)	19.4	23.2	ASTMD 638-02
Tensile modulus (GPa)	0.92	33.3	ASTMD 638-02
Flexural strength (MPa)	22.6	—	ASTMD 790-03
Flexural modulus (GPa)	0.896	41.9	ASTMD 790-03
Rockwell hardness	136.1	1.32	ASTMD1525-01
Brittle temperature (°C)	-39	151.3	ASTMD 746-98
Heat deformation (0.45 MPa) (°C)	127.4	115.2	ASTMD 648-01

with common PP. This was because of the incorporation of EPR in PP matrix. The data shown in Table II indicated that the EPR obtained during in situ blending contains polymer chains of variable composition with a distribution of ethylene and propylene sequence lengths. The sequence lengths of copolymer included noncrystallizable short blocks and those of long enough to crystallize as lamellae. The results in Table II indicate that copolymer contains more propylene segment with long sequences. It is most likely due to the fact that a certain amount of low-molecular-weight PP homopolymer and atactic PP were extracted.

#### Morphology evaluation of HIPP by SEM

It is well known that particle size and dispersity of EPR have important influences on the physical and mechanical properties of the HIPP.<sup>14</sup> The rubbery phase must be homogeneously dispersed and its size should be well controlled to achieve the best stiffness-toughness balance. Figure 2 shows that there are many micro-pores being existed in the homopolypropylene, while EPR are filled in such micro-pores in the case of copolymer (see Fig. 3). The particle size of the EPR is smaller than 1  $\mu\text{m}$ . The final product after two stages of reaction is still free flowing, spherical granules. This means that most of the copolymer has been formed inside the granules. After being injection molded and brittle ruptured at  $-23^\circ\text{C}$ , the obtained HIPP was

etched by xylene at  $25^\circ$  and  $80^\circ\text{C}$ , respectively, and then cut into sections for SEM observation (as shown in Figs. 4 and 5, respectively). Comparing these two SEM pictures, it is clear that there are still some residual polymers not to be removed by xylene etching at  $25^\circ\text{C}$  (as shown in Fig. 4). It should be block copolymer of ethylene and propylene that is insoluble in xylene at  $25^\circ\text{C}$ . It functions as a compatibilizer between matrix and EPR. We can see from Figure 5 that most of the block copolymer were extracted by xylene at  $80^\circ\text{C}$ . Particle size of the EPR (plus *a*-PP) is larger than 1  $\mu\text{m}$  after injection molding. Comparing the particle dispersions before and after injection molding, a considerable increase in the EPR particle size can be observed. It shows that the EPR dispart from matrix during the injection molding, resulting in the increase of the EPR particle size.

#### Morphology evaluation of HIPP by AFM

AFM overcomes the prerequisite for a conducting coating, and it can provide topographical information on dimension scales that are inaccessible to SEM or TEM.<sup>15</sup> The AFM images of HIPP (as shown in Fig. 6) indicated that the EPR, being dark particles of 1  $\mu\text{m}$  or larger in diameter, was well-dispersed within a polypropylene matrix. Area analysis of lower magnification images confirms the 14.3 wt % EPR formulation. It is in accordance with the results of FTIR determination. The images of AFM suggest that the EPR

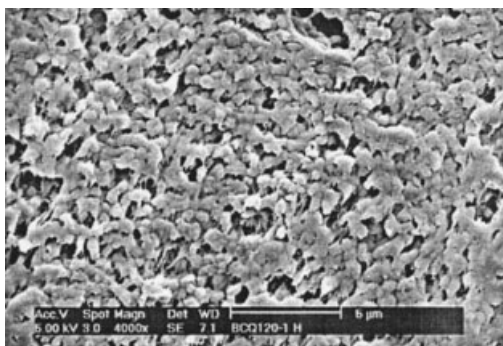


Figure 2 Section SEM picture of homopolymer.

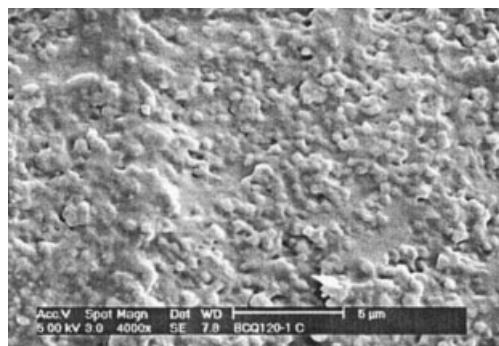


Figure 3 Section SEM picture of copolymer.



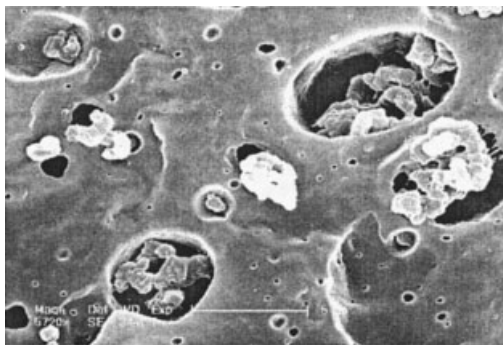


Figure 4 The section SEM picture of the HIPP after pelleting being etched by xylene at 25°C.

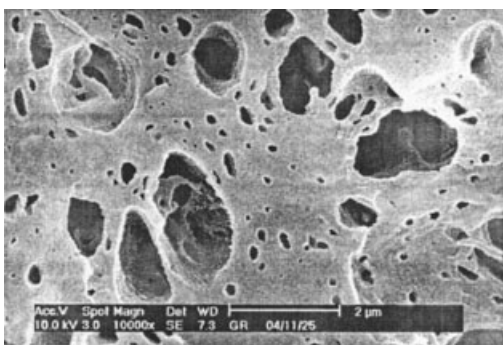


Figure 5 The section SEM picture of the HIPP after pelleting being etched by xylene at 80°C.

phase exit in HIPP as both large elongated particles and long thin rods. It can be presumed that the large elongated particles contain crystalline fractions, while the long thin one consists of amorphous chains.

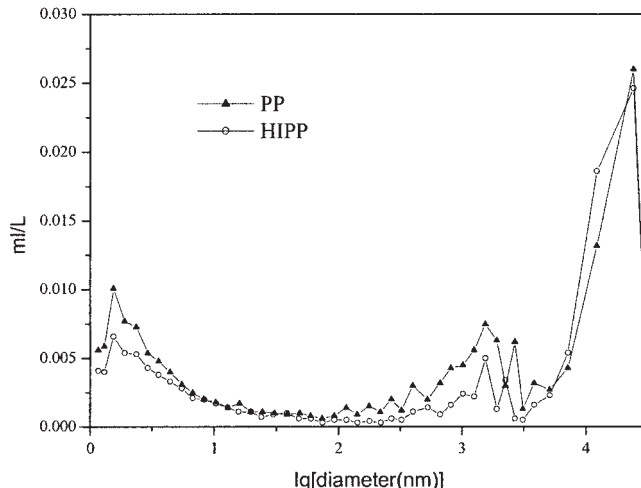


Figure 7 Pore structure of homopolymer and copolymer.

**Pore structure evaluation of HIPP by mercury intrusion**

The pore characterization of homopolypropylene and HIPP were determined by mercury intrusion and shown in Figure 7. From the pore distribution curve of the copolymer, it is concluded that there are some micro-pores in copolymer particle, especially pore diameter less than 10 nm. Comparing the pore structure of homopolymer and copolymer, we can draw a conclusion that the homopolymer with pore diameter between 100 and 10,000 nm are suitable for EPR to fill in. The results tell us that mass transfer limitations in ethylene-propylene copolymerization exist. It prevents the feeds stock from getting into micro-pore.<sup>16</sup>

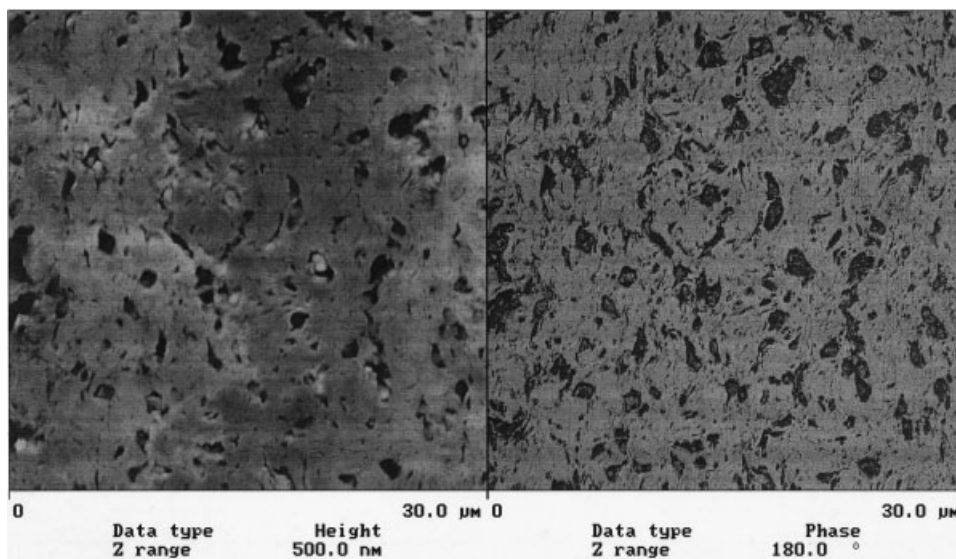


Figure 6 Phase-imaging AFM of the copolymer (shading is representative of EPR).

### CONCLUSIONS

The HIPP has been prepared by in situ blending of polypropylene and EPR with spherical Ziegler–Natta catalyst. The composition, morphology, and pore characterization of such HIPP were investigated by xylene extraction, SEM, AFM, and mercury intrusion. The results showed that EPR was composed of amorphous copolymer and ethylene–propylene block copolymer. The block copolymer fractions function as a compatibilizer that localize at the interface between matrix and EPR. Controlling the pore diameter of homopolypropylene is important for HIPP with high content of EPR.

### References

1. Galli, P.; Vecellio, G. *J Polym Sci Part A: Polym Chem* 2004, 42, 396.
2. Moore, E. P. *Polypropylene Handbook*; Hanser: Munich, 1996.
3. Fan, Z. Q.; Zhang, Y. Q.; Xu, J. T. *Polymer* 2001, 42, 5559.
4. Covezzi, M.; Mei, G. *Chem Eng Sci* 2001, 56, 4059.
5. Cai, H. J.; Luo, X. L.; Ma, D. Z. *J Appl Polym Sci* 1999, 71, 931.
6. Feng, Y.; Hay, J. N. *Polymer* 1998, 39, 6723.
7. Besombes, M.; Menguel, J. F.; Delmas, G. *J Polym Sci Part B: Polym Phys* 1988, 26, 1881.
8. Mckenna, T. F.; Bouzid, D. K.; Matsunami, S. *Polym React Eng* 2003, 11, 177.
9. Debling, J. A.; Ray, W. H. *J Appl Polym Sci* 2001, 81, 3085.
10. Kittilsen, P.; Mckenna, T. F. *J Appl Polym Sci* 2001, 82, 1047.
11. Carlos, A. C.; Sebastao, V. C. *Mater Res* 2000, 3, 37.
12. Fu, Z. S.; Fan, Z. Q.; Zhang, Y. Q. *Eur Polym J* 2003, 39, 795.
13. Randall, J. C. *J Polym Sci Part A: Polym Chem* 1998, 36, 1527.
14. Paula, P.; Daniel, E.; Graciela, G. *J Elastomers Plastics* 2002, 34, 131.
15. Valery, V. P.; Kohhei, N.; Minoru, T. *Macromol Chem Phys* 2004, 205, 179.
16. Pires, M.; Mauler, R. S.; Liberman, S. A. *J Appl Polym Sci* 2004, 92, 2155.